Ab initio calculation of the frequency-dependent interaction induced hyperpolarizability of Ar_2

Berta Fernández
Department of Physical Chemistry, Faculty of Chemistry, University of Santiago de Compostela, E-15706 Santiago de Compostela, Spain

Christof Hättig
Department of Chemistry, University of Aarhus, DK-8000 Aarhus C, Denmark

Henrik Koch
Department of Chemistry, University of Odense, DK-5230 Odense M, Denmark

Antonio Rizzo[a)]
Istituto di Chimica Quantistica ed Energetica Molecolare del Consiglio Nazionale delle Ricerche, Via Risorgimento 35, I-56126 Pisa, Italy

(Received 17 September 1998; accepted 3 November 1998)

The frequency-dependent interaction induced polarizability and second hyperpolarizability of the argon dimer are computed for a range of internuclear distances employing the coupled cluster singles and doubles response approach. The frequency dependence of the interaction-induced properties is treated through second order in the frequency arguments using expansions in Cauchy moments and hyperpolarizability dispersion coefficients. The dielectric, the refractivity, the Kerr and the hyperpolarizability second virial coefficients are computed for a range of temperatures employing a recent accurate *ab initio* potential for the ground state of the argon dimer. For most of the computed virial coefficients good agreement is obtained between the present *ab initio* results and the available experimental data. © *1999 American Institute of Physics.* [S0021-9606(99)00306-2]

I. INTRODUCTION

The interest in nonlinear optical effects has increased considerably in the last few years, and there has been much effort in the experimental and theoretical determination of polarizabilities and hyperpolarizabilities. With the improvement of the experimental and the theoretical techniques to provide reliable data for linear and nonlinear optical properties, accurate extrapolations of the experimental gas phase data are crucial, therefore the pressure or density dependence of these properties is important.

Experimentally, the determination of virial coefficients for electric and optical properties is not an easy task.[1–13] In the most recent study, the second dielectric virial coefficient of argon $B_\epsilon(T)$ was measured for several temperatures by Huot and Bose.[11] Previous measurements are due to Vidal and Lallemand,[5] Bose *et al.*,[3,9] Johnston *et al.*,[1] Orcutt and Cole[2] and Proffitt *et al.*[7] Buckingham and Graham[4], Burns *et al.*,[8] Coulon *et al.*,[6] Achtermann *et al.*[10] and Hohm[13] determined the second refractivity virial coefficient $B_R(\omega,T)$. The second Kerr virial coefficient $B_K(\omega,T)$ has been estimated among others by Dunmur *et al.*,[14,15] Buckingham and Dunmur,[16] and recently by Shelton and Palubinskas.[17]

The effect of internuclear interaction on the electric field induced second harmonic generation (ESHG) hyperpolarizability has caused some uncertainty in the literature[12,18,19] about the precision of recent accurate gas phase measurements[18,20–26] of the ESHG hyperpolarizabilities of some small molecules and atoms. In ESHG experiments the second hyperpolarizability of a gas is usually measured as a ratio relative to a reference gas with a very accurately known hyperpolarizability. Recently, Donley and Shelton[12] measured the hyperpolarizability ratios $\gamma_\parallel^{\mathrm{ESHG}}(\mathrm{Ar})/\gamma_\parallel^{\mathrm{ESHG}}(\mathrm{H_2})$, $\gamma_\parallel^{\mathrm{ESHG}}(\mathrm{N_2})/\gamma_\parallel^{\mathrm{ESHG}}(\mathrm{H_2})$ and $\gamma_\parallel^{\mathrm{ESHG}}(\mathrm{H_2})/\gamma_\parallel^{\mathrm{ESHG}}(\mathrm{He})$, as a function of the density with a 0.1% accuracy at a wavelength of 514.5 nm. The pressure dependence of these ratios accounts, however, for no more than a few tenths of a percent of the total results, thus making an accurate determination of the virial coefficients difficult. From a plot of four measurements for each of the ratios versus the H_2 gas density Donley and Shelton determined the first-order density corrections for the three ratios as $-7.0\pm5.0\times10^{-6}$, $-6.9\pm4.6\times10^{-6}$, and $+5.6\pm6.2\times10^{-6}$ $\mathrm{m^3\ mol^{-1}}$, respectively. They made a theoretical estimation for the second virial coefficients of the ESHG hyperpolarizability ratios using the dipole-induced dipole (DID) model and a Lennard-Jones 6–12 potential. The authors found such a model incapable of providing quantitative estimates for the properties. Although it predicts the correct order of magnitude of the effect, the hyperpolarizability virial coefficients are obtained with the wrong sign.

The DID model and its variations are the most common approximations used to model interaction induced polarizabilities within a classical multipolar treatment of intermolecular interactions.[27–32] The model considers the atomic polarizabilities independent of the internuclear distance, but takes into account the fact that each atom responds to the sum of the external and the induced dipole moment fields.[12,31] Using this, Godfried and Silvera[33] reproduced the

a)Electronic mail: rizzo@hal.icqem.pi.cnr.it

 © 1999 American Institute of Physics

rotational Raman spectra of the argon dimer within the (rather large) experimental uncertainty. This demonstrates that the DID model includes the most important contribution to the interaction induced polarizability anisotropy, which is much larger and easier to model than the isotropic (or trace) polarizability and the hyperpolarizability.

The theoretical determination of second virial coefficients for linear and nonlinear optical properties is a challenging task even for modern *ab initio* methods because it combines the difficulties faced in the *ab initio* calculation of the weak intermolecular interaction with those of the computation of electric or optical properties.

A calculation of the interaction-induced hyperpolarizability of the helium dimer was carried out recently by Bishop and Dupuis.[34] They used fourth-order Møller–Plesset perturbation theory (MP4) as the highest correlation level and a $[12s5p3d2f/6s5p3d2f]$ basis set. For the dielectric virial coefficient good agreement with the experimental value and a previous theoretical configuration interaction singles and doubles (CISD) determination[35] was obtained. For the second virial coefficient of the second hyperpolarizability of helium experimental determinations are not available. However, using their helium result and data for the density dependence of the hyperpolarizability ratios taken from Ref. 12 the authors estimated the second virial coefficient of the second electric hyperpolarizability of H_2, N_2 and Ar.

Joslin *et al.*[36] evaluated the interaction polarizability of the argon dimer at different internuclear distances using second-order Møller Plesset theory (MP2) and a $[18s14p6d]$ basis set, an extension of the set employed by Dacre in his self-consistent field (SCF) study.[37] Among other properties they obtained the second dielectric, the second refractivity and the second Kerr virial coefficients as a function of the temperature. As expected, electron correlation effects are crucial to describe these properties, and the MP2 results are still far from the experimental stage.[10,11] This discrepancy was justified in terms of a possible error in the experimental determinations. Previous calculations were in disagreement between each other and with the experiment.[10,11]

Since the interaction-induced properties are obtained as rather small corrections to the corresponding optical properties of the noninteracting monomers, high-level response approaches, able to deal efficiently with electron correlation, are required for their computation. Another necessary condition, not met by all correlated response approaches,[38–40] is that the computed optical properties must be size extensive. A method which meets these requirements is the coupled cluster (CC) response approach, which is known to yield precise values for a large number of molecular properties. The CC response approach has recently been extended within the hierarchy of coupled cluster singles (CCS), coupled cluster iterative second order (CC2) and coupled cluster singles and doubles (CCSD) to provide dynamic third- and fourth-order properties, therefore allowing the evaluation of highly accurate frequency-dependent polarizabilities and hyperpolarizabilities.[41–43] Another important issue for the *ab initio* calculation of interaction induced polarizabilities and hyperpolarizabilities is the choice of the one-particle basis set: as demonstrated by the basis set study presented in Secs. III and IV, extended, high-quality basis sets are required to obtain accurate results, in particular for the isotropic interaction-induced hyperpolarizability.

In the present study the frequency-dependent interaction induced polarizability and second hyperpolarizability of the Ar_2 are computed as a function of the internuclear distance at the CCSD level. We perform the calculations in a systematic way, starting with a basis set study of the static limit using Dunning's correlation consistent polarized valence basis sets.[44–48] For the selected basis set the polarizability and the second hyperpolarizability are then calculated as a function of the internuclear distance. The dispersion of the properties is thereby included through second order in the frequency arguments by means of the $S(-4)$ Cauchy moment[49] for the linear polarizability and the A coefficient[50] for the second hyperpolarizability. The dielectric, the refractivity, the Kerr and the second hyperpolarizability second virial coefficients are calculated from these results employing a recent accurate *ab initio* Ar_2 ground state potential.[51] The latter was obtained at the CCSD with perturbative treatment of triples [CCSD(T)] level using a d-aug-cc-pV5Z basis set including midbond functions. In Ref. 52 this potential was shown to describe the Ar_2 rovibronic spectrum very accurately.

Section II gives a brief summary of the equations used in the computation of the interaction-induced dynamic polarizabilities and hyperpolarizabilities and for the calculation of the second virial coefficients. In Sec. III the computational details of the CCSD calculations and of the numerical integration entering in the expressions for the virial coefficients are given. The results for the various properties are presented and discussed in Sec. IV and our concluding remarks are given in Sec. V.

II. THEORY

The present study deals with the changes of the frequency-dependent polarizability and hyperpolarizability of Ar induced by the pair interaction with other Ar atoms. Since we employ standard *ab initio* approximations and expand in basis sets the wave functions, from which the properties are calculated, we have to account for basis set superposition errors. This is done using the counterpoise procedure advocated by Boys and Bernardi,[52] a standard procedure for the calculation of interaction energies for van der Waals molecules. It can be generalized for the calculation of counterpoise corrected interaction-induced properties as

$$\Delta P(\mathbf{R}) = P_{A-B}(S_{A-B}|\mathbf{R}) - P_A(S_{A-B}|\mathbf{R}) - P_B(S_{A-B}|\mathbf{R}), \quad (1)$$

where $P_{A-B}(S_{A-B}|\mathbf{R})$ is the property of the dimer evaluated in the dimer basis set S_{A-B} at the geometry $\mathbf{R}$ and $P_A(S_{A-B}|\mathbf{R})$ and $P_B(S_{A-B}|\mathbf{R})$ are the properties of the monomers A and B, respectively, evaluated in the dimer basis set for the same geometry. For the homonuclear argon dimer $P_A(S_{A-B}|\mathbf{R}) = P_B(S_{A-B}|\mathbf{R})$. In the following, we study the isotropic electric dipole polarizability

$$\alpha_{\text{ave}} = \tfrac{1}{3}(2\alpha_{xx} + \alpha_{zz}), \quad (2)$$

the polarizability anisotropy

$$\alpha_{\text{ani}} = \alpha_{zz} - \alpha_{xx}, \quad (3)$$

and the isotropic parallel average of the second electric dipole hyperpolarizability

$$\gamma_{\parallel}=\frac{1}{15}\sum_{\xi\eta}\left(\gamma_{\xi\xi\eta\eta}+\gamma_{\xi\eta\xi\eta}+\gamma_{\xi\eta\eta\xi}\right). \tag{4}$$

Note that we use the subscripts ave and ani to indicate the isotropic average and the anisotropy and $\Delta\alpha$ for the interaction induced polarizability to avoid conflicts with the notation used for hyperpolarizabilities. Other authors employ $\Delta\gamma$ (see Ref. 36) or β (see Refs. 35 and 37) to indicate the interaction-induced anisotropy of the electric dipole polarizability.

In order to perform a comparison with experimental data for the virial coefficients of the polarizability and hyperpolarizability, we must calculate $\Delta\alpha_{\rm ave}$, $\Delta\alpha_{\rm ani}$ and $\Delta\gamma_{\parallel}$ as functions of the internuclear distance. Furthermore, as these properties are frequency dependent, their accurate calculations as a function of both the internuclear distance and the frequency would be prohibitive and approximations are needed. Thus, the dispersion of the interaction-induced properties is truncated to second order in the power series expansion in the frequency arguments. The power series expansion of the polarizability

$$\alpha(\omega)=\sum_{k=0}^{\infty}\omega^{2k}S(-2k-2)=\alpha(0)+\omega^2S(-4)+\ldots, \tag{5}$$

is also known as the Cauchy series. The $S(k)$ are the so-called Cauchy moments and $S(-2)=\alpha(0)$. For the isotropic parallel average of the second hyperpolarizability $\gamma_{\parallel}$ we use a dispersion formula originally proposed by Shelton[21]

$$\gamma_{\parallel}(\omega_0;\omega_1,\omega_2,\omega_3)=\gamma_{\parallel}(0)(1+\omega_L^2A+\ldots), \tag{6}$$

where the coefficient A is independent of the nonlinear optical process: $\omega_0=-\omega_1-\omega_2-\omega_3$ and $\omega_L^2=\omega_0^2+\omega_1^2+\omega_2^2+\omega_3^2$. The Cauchy moments $S(-4)$ and the coefficient A are evaluated as analytic derivatives[53,54]

$$S(-4)=\frac{1}{2}\left(\frac{d^2\alpha(\omega)}{d\omega^2}\right)_{\omega=0}, \tag{7}$$

$$\gamma_{\parallel}(0)A=\frac{1}{2}\left(\frac{d^2\gamma_{\parallel}(\omega_0;\omega_1,\omega_2,\omega_3)}{d\omega_L^2}\right)_{\omega_L=0}. \tag{8}$$

The interaction-induced isotropic polarizability $\Delta\alpha_{\rm ave}(\omega,R)$ is related to the second refractivity virial coefficient $B_R(\omega,T)$ and is important for the description of the intensities in isotropic collision-induced light scattering (CILS) spectra.[36] The second refractivity virial coefficient is obtained from the expansion of the generalization of the Clausius–Mossotti function in orders of the molar density ρ (the inverse molar volume) of the gas

$$\frac{n^2-1}{n^2+2}=A_R(\omega,T)\rho+B_R(\omega,T)\rho^2+C_R(\omega,T)\rho^3+\ldots, \tag{9}$$

where n is the refractive index. For atoms the virial coefficient $A_R(\omega,T)$ is directly related to the atomic polarizability

$$A_R(\omega,T)=\frac{N_A}{3\epsilon_0}\alpha_{\rm ave}(\omega), \tag{10}$$

where N_A is Avogadro's number, and ϵ_0 is the vacuum permittivity. For thermal energies kT large compared to the dissociation energy of the argon dimer (99.5 $\rm cm^{-1}$),[55,56] i.e., for $T>143$. K, the second refractivity virial coefficient can be calculated from the classical statistical mechanics expression[57]

$$B_R(\omega,T)=\frac{N_A^2}{6\epsilon_0}X_{\alpha_{\rm ave}}(\omega,T), \tag{11}$$

$$X_{\alpha_{\rm ave}}(\omega,T)=4\pi\int_0^{\infty}\Delta\alpha_{\rm ave}(\omega,R)\times\exp[-V(R)/kT]R^2\,dR, \tag{12}$$

where $V(R)$ is the interatomic potential of the argon dimer. For very low temperatures with kT comparable to or smaller than the dissociation energy of the dimer quantum corrections, which account for the discrete vibrational levels of the van der Waals molecule, must be included.[58,59] In the present study we assume that the classical approximation can be used, and we approximate the frequency dependence of the refractivity virial coefficient by expanding it in a power series in ω to second order

$$B_R(\omega,T)=B_R^{(0)}(T)+\omega^2B_R^{(2)}(T)+\ldots, \tag{13}$$

where the static limit $B_R^{(0)}(T)$ is identical to the second dielectric virial coefficient $B_\epsilon(T)$.[60] The coefficients $B_R^{(0)}(T)$ and $B_R^{(2)}(T)$ are calculated analogous to Eqs. (11) and (12), but with $\Delta\alpha_{\rm ave}(\omega,R)$ replaced by the interaction-induced static polarizability and the Cauchy moment $\Delta\alpha_{\rm ave}(0,R)$ and $\Delta S_{\rm ave}(-4,R)$, respectively.

The interaction-induced polarizability anisotropy $\Delta\alpha_{\rm ani}(\omega,R)$ is related to the depolarized light intensity in CILS spectra and to the pressure dependence of the dc Kerr or electro-optical effect. The latter is conveniently expressed by an expansion of the molar Kerr constant ${}_mK$ as a power series in the density[16]

$${}_mK(\omega,T)=A_K(\omega,T)+B_K(\omega,T)\rho+C_K(\omega,T)\rho^2+\ldots, \tag{14}$$

where for atoms the first Kerr virial coefficient A_K is related to the dc Kerr hyperpolarizability $\gamma_K(\omega)$:

$$A_K(\omega)=\frac{N_A}{81\epsilon_0}\gamma_K(\omega). \tag{15}$$

The second Kerr virial coefficient $B_K(\omega,T)$ contains contributions related to the interaction-induced polarizability and hyperpolarizability such that

$$B_K(\omega,T)=\frac{N_A^2}{162\epsilon_0}\left(\frac{1}{5kT}X_K^{\alpha}(\omega,T)+X_K^{\gamma}(\omega,T)\right)=B_K^{\alpha}(\omega,T)+B_K^{\gamma}(\omega,T). \tag{16}$$

Here k is the Boltzmann constant. For homonuclear dimers within the classical statistical mechanics treatment, $X_K^{\alpha}(\omega,T)$ is obtained as[16,60]

$$X_K^{\alpha}(\omega,T)=4\pi\int_0^{\infty}\Delta\alpha_{\mathrm{ani}}(\omega,R)\Delta\alpha_{\mathrm{ani}}(0,R)\times\exp[-V(R)/kT]R^2\,dR. \quad (17)$$

Again, we expand $X_K^{\alpha}(\omega,T)$ as a power series in ω to second order and evaluate the coefficients by replacing $\Delta\alpha_{\mathrm{ani}}(\omega,R)$ with the induced static polarizability anisotropy $\Delta\alpha_{\mathrm{ani}}(0,R)$ and the $\Delta S_{\mathrm{ani}}(-4,R)$ Cauchy moment. The hyperpolarizability contribution to the pressure dependence of the Kerr constant is usually small and is often neglected in the analysis of experimental results.[16] Within the classical statistical mechanics approximation X_K^{γ} can be computed analogous to $X_{\alpha_{\mathrm{ave}}}(\omega,T)$ as

$$X_K^{\gamma}(\omega,T)=4\pi\int_0^{\infty}\Delta\gamma_K(\omega,R)\exp[-V(R)/kT]R^2\,dR. \quad (18)$$

Since $B_K^{\gamma}(\omega,T)$, and in particular its dispersion contribution, make only a small correction to the dominant term $B_K^{\alpha}(\omega,T)$, we assumed the validity of the Kleinman symmetry[61] in the calculation of $X_K^{\gamma}(\omega,T)$ (see Sec. III) and thus $\Delta\gamma_K(\omega,R)\approx\Delta\gamma_{\parallel}(\omega,R)$. This relation is exact in the static limit but an (often very good) approximation for the frequency-dependent part.

For atoms the interaction-induced hyperpolarizability is the only property contributing to the pressure dependence of some other third-order nonlinear optical effects, in particular of the ESHG. Following the general treatment of Buckingham and Pople,[60] we introduce for the second hyperpolarizability the virial expansion

$$\gamma(\Omega,\rho,T)=\gamma(\Omega)+B_{\gamma}(\Omega,T)\rho+\ldots, \quad (19)$$

where Ω is a shorthand notation for the usual sequence $\omega_0;\omega_1,\omega_2,\omega_3$ of frequencies and the coefficient $B_{\gamma}(\Omega,T)$ within the semiclassical approximation is given by

$$B_{\gamma}(\Omega,T)=\frac{N_A}{2}X_{\gamma}(\Omega,T), \quad (20)$$

with

$$X_{\gamma}(\Omega,T)=4\pi\int_0^{\infty}\Delta\gamma_{\parallel}(\Omega,R)\exp[-V(R)/kT]R^2\,dR. \quad (21)$$

Since in ESHG experiments the hyperpolarizability of a gas, and thus its pressure dependence, can only be measured relative to that of a second reference gas, for comparison with the experiment Eq. (19) is rewritten as[12]

$$\frac{\gamma_A(\Omega,\rho_A,T)}{\gamma_B(\Omega,\rho_B,T)}=\frac{\gamma_A(\Omega)}{\gamma_B(\Omega)}[1+b(AB)\rho_{\mathrm{ref}}], \quad (22)$$

with

$$b(AB)=\left(b_A(\Omega,T)-b_B(\Omega,T)\frac{\rho_B}{\rho_A}\right)\frac{\rho_A}{\rho_{\mathrm{ref}}}, \quad (23)$$

and ρ_{ref} being the density of the reference gas and $b_A(\Omega,T)$, $b_B(\Omega,T)$ the second hyperpolarizability virial coefficients divided by the hyperpolarizability of the isolated atoms, i.e., $B_{\gamma,A}(\Omega,T)/\gamma_A(\Omega)$. As for the interaction-induced polarizabilities, we treat the frequency dependence of $\gamma_{\parallel}$ and $\Delta\gamma_{\parallel}$ approximately by using the power series in Eq. (6) through second order in the frequencies

$$B_{\gamma}(\Omega,T)=B_{\gamma}^{(0)}(T)+\omega_L^2B_{\gamma}^{(2)}(T)+\ldots, \quad (24)$$

$$b(\Omega,T)=\frac{B_{\gamma}^{(0)}(T)+\omega_L^2B_{\gamma}^{(2)}(T)+\ldots}{\gamma_{\parallel}(0)(1+\omega_L^2A+\ldots)}. \quad (25)$$

III. COMPUTATIONAL DETAILS

The polarizabilities, Cauchy moments, hyperpolarizabilities, and hyperpolarizability dispersion coefficients are calculated using the coupled cluster response approach[42,62] and CCSD wave functions. The coupled cluster calculations are carried out using the integral-direct coupled cluster program described in Refs. 42, 54, 55, 63, and 64, which is a part of the DALTON program package.[65]

In the CCSD response calculations we have frozen the $1s^22s^22p^6$ orbitals of the argon atoms. All results for the interaction-induced properties reported in the following are counterpoise corrected using the method of Boys and Bernardi.[52]

The selection of the basis set and the estimation of the remaining basis set error is one of the most crucial steps in the *ab initio* calculation of interaction-induced electric properties. Therefore, we perform a basis set study for the static interaction-induced polarizability and hyperpolarizability at the experimental equilibrium distance of the argon dimer (7.10 a.u.).[56] Two series of basis sets are employed in the basis set study: the correlation consistent basis sets x-aug-cc-pVXZ, (x=d,t,q; X=D,T,Q,5), developed by Dunning and co-workers,[44–48] and a series where these basis sets are extended with an uncontracted $(3s3p2d1f1g)$ set of midbond functions,[51] denoted as x-aug-cc-pVXZ-33211. To investigate the possible differences in basis set requirements with respect to the internuclear distance, we perform calculations at two distances using two of the above mentioned basis sets. The results of the basis set study are summarized in Tables I and II. The final calculations of the interaction-induced po-

TABLE I. Ar_2. Basis set study (in a.u.) part I ($R=7.10$ a.u.).

Basis set	$\Delta\alpha_{\mathrm{ave}}$	$\Delta\gamma_{\parallel}$
d-aug-cc-pVDZ	−0.0206	−54.5548
d-aug-cc-pVTZ	0.0001	−38.4548
d-aug-cc-pVQZ	0.0062	−33.8080
d-aug-cc-pV5Z	0.0087	−33.6102
d-aug-cc-pVDZ-33211	0.0039	−29.1446
d-aug-cc-pVTZ-33211	0.0058	−32.5514
d-aug-cc-pVQZ-33211	0.0081	−32.9991
d-aug-cc-pV5Z-33211	0.0095	−33.6141
t-aug-cc-pVDZ-33211	0.0037	−30.2349
t-aug-cc-pVTZ-33211	0.0065	−38.3879
t-aug-cc-pVQZ-33211	0.0085	−35.3084
t-aug-cc-pV5Z-33211	0.0096	−33.6990
q-aug-cc-pVDZ-33211	0.0039	−29.3794
q-aug-cc-pVTZ-33211	0.0067	−38.3496

TABLE II. Ar_2. Basis set study (in a.u.) part II.

Basis set	R (a.u.)	$\Delta\alpha_{ave}$	$\Delta S_{ave}(-4)$	$\Delta\gamma_{\|}$	$\Delta(\gamma_{\|}\times A)$
d-aug-cc-pVTZ-33211	7.0	0.0009	−0.2141	−37.46	−409.0
t-aug-cc-pVQZ-33211	7.0	0.0040	−0.1785	−40.04	−592.1
d-aug-cc-pVTZ-33211	10.0	0.0107	0.0877	10.99	65.93
t-aug-cc-pVQZ-33211	10.0	0.0108	0.0858	7.98	50.37

larizabilities and hyperpolarizabilities as a function of the interatomic distance as needed for the computation of the integrals in Eqs. (12), (17), (18) and (21) are carried out using the d-aug-cc-pVTZ-33211 basis set. The results for $\Delta\alpha_{ave}$, $\Delta S_{ave}(-4)$, $\Delta\alpha_{ani}$, $\Delta S_{ani}(-4)$, $\Delta\gamma_{\|}$ and $\Delta(\gamma_{\|}A)$ at 31 different internuclear distances between 5 and 30 a.u. are collected in Table III.

The ground state potential of the argon dimer is taken from the recent work of Fernández and Koch.[52] This CCSD(T) potential was evaluated using a d-aug-cc-pV5Z basis set extended with a $(3s3p2d1f1g)$ set of midbond functions (d-aug-cc-pV5Z-33211), consisting in total of 372 basis functions for Ar_2. It was available for a total of 59 internuclear distances in the range between 3.8 and 20.0 a.u. and it is expected to be the most accurate *ab initio* potential for Ar_2 available at present. To interpolate between the points of the potential we use a cubic spline fit. The other terms in the

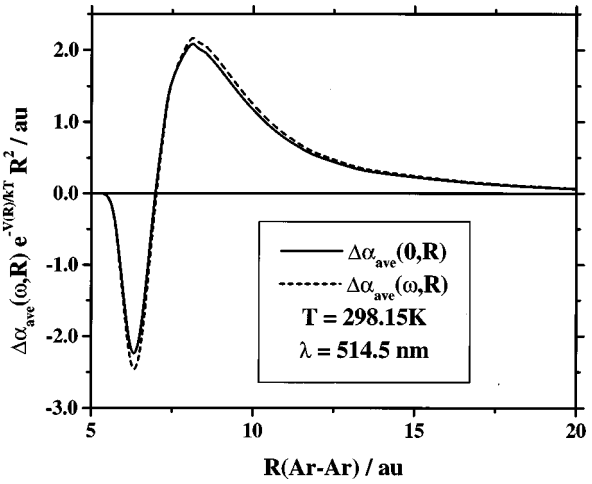


FIG. 1. Ar_2. The function $\Delta\alpha_{ave}(\omega,R)e^{-V(R)/kT}R^2$ (a.u.) against the interatomic distance R (a.u.) for $T=298.15$ K and $\lambda=514.5$ nm.

integrands of the equations are then computed for each of the interatomic distances listed in Table III, cubic spline fitted, separating the frequency-independent and frequency-dependent contribution to the integrals, and finally interpolated at a total of 500 points between 5 and 30 a.u. The functions to be numerically integrated, computed for $T=298.15$ K, are shown in Figs. 1–4. Figure 1 displays the

TABLE III. Ar_2. The dependence on the interatomic distance *(R)* of the relevant properties (a.u.). d-aug-cc-pVTZ-33211 basis set.

R	$\Delta\alpha_{ave}$	$\Delta S_{ave}(-4)$	$\Delta\alpha_{ani}$	$\Delta S_{ani}(-4)$	$\Delta\gamma_{\|}$	$\Delta(\gamma_{\|}\times A)$
5.00	−0.348 22	−2.110 81	3.876 21	16.683 33	21.5768	715.9981
5.10	−0.326 43	−2.100 09	3.717 11	15.816 42	−8.7474	376.9389
5.25	−0.29000	−2.017 20	3.508 18	14.760 07	−41.9262	−1.8658
5.50	−0.226 32	−1.768 69	3.216 11	13.455 65	−73.3290	−389.4657
5.75	−0.166 26	−1.457 50	2.968 70	12.504 43	−84.7766	−578.5512
6.00	−0.114 31	−1.138 47	2.747 95	11.746 55	−83.8663	−644.3837
6.25	−0.072 10	−0.843 18	2.544 12	11.086 73	−75.6835	−633.8051
6.50	−0.039 57	−0.587 78	2.352 47	10.471 02	−63.7504	−577.9326
6.75	−0.015 72	−0.378 27	2.171 18	9.872 52	−50.4854	−498.1287
7.00	0.000 87	−0.214 07	1.999 97	9.281 16	−37.4634	−408.9977
7.25	0.011 71	−0.090 81	1.839 21	8.696 36	−25.6280	−320.2296
7.50	0.018 20	−0.002 36	1.689 32	8.122 00	−15.4673	−237.8760
8.00	0.022 71	0.096 02	1.422 78	7.026 18	−0.6558	−104.0331
8.25	0.022 45	0.117 63	1.305 83	6.514 65	4.1896	−54.1832
8.50	0.021 30	0.127 25	1.199 20	6.032 31	7.6076	−15.0949
8.60	0.020 68	0.128 59	1.159 30	5.848 05	8.6312	−2.2210
8.75	0.019 65	0.128 56	1.102 28	5.581 25	9.8482	14.3983
9.00	0.017 77	0.124 43	1.014 39	5.162 37	11.1561	35.6916
9.50	0.013 98	0.107 70	0.862 76	4.419 85	11.8230	59.3076
10.00	0.010 68	0.087 67	0.738 57	3.795 65	10.9884	65.9264
10.50	0.008 05	0.069 12	0.636 58	3.274 75	9.5349	63.1990
11.00	0.006 06	0.053 67	0.552 38	2.840 82	7.9552	56.1617
11.50	0.004 60	0.041 50	0.482 40	2.478 66	6.4905	47.8076
12.00	0.003 53	0.032 19	0.423 82	2.175 14	5.2339	39.7054
13.00	0.002 17	0.019 90	0.332 49	1.702 46	3.3744	26.5266
14.00	0.001 44	0.012 90	0.265 78	1.358 40	2.2034	17.6289
16.00	0.000 71	0.006 05	0.177 68	0.906 05	0.9863	8.0461
18.00	0.000 34	0.002 85	0.124 55	0.634 27	0.4445	3.7224
20.00	0.000 16	0.001 31	0.090 68	0.461 25	0.1962	1.6885
22.00	0.000 08	0.000 66	0.068 07	0.346 05	0.0878	0.7630
30.00	0.000 01	0.000 10	0.026 82	0.136 28	0.0091	0.0760

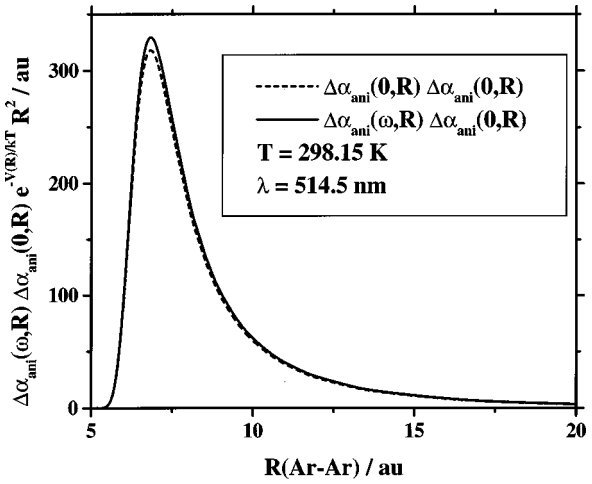


FIG. 2. Ar_2. The function $\Delta\alpha_{\mathrm{ani}}(0,R)\Delta\alpha_{\mathrm{ani}}(\omega,R)e^{-V(R)/kT}R^2$ (a.u.) against the interatomic distance R (a.u.), for $T=298.15$ K and $\lambda=514.5$ nm.

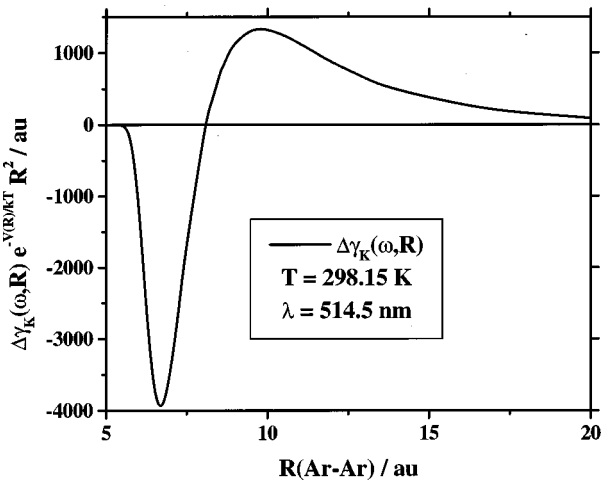


FIG. 3. Ar_2. The function $\Delta\gamma_K(\omega,R)e^{-V(R)/kT}R^2$ (a.u.) against the interatomic distance R (a.u.) for $T=298.15$ K and $\lambda=514.5$ nm.

behavior of the integrand in Eq. (12) in the 5–20 a.u. internuclear distance range for the wavelength of 514.5 nm, i.e., the frequency of Donley and Shelton's experimental work.[12] Both the frequency-independent and frequency-dependent contribution to the integrand are shown. Figures 2, 3 and 4 show the behavior of the integrands in Eqs. (17), (18) and (21), respectively. The numerical integration, which covers the 5–30 a.u. range, leads to the results shown in the next sections. It is quite evident from Figs. 1–4 that the contribution to the integral over the interatomic distance is completely negligible below 5 a.u. This is true for the whole range of temperatures chosen in this work. As T increases, the importance of regions at low interatomic distances and in particular below 5 a.u. increases dramatically, to the point where our set of data becomes insufficient to provide accurate values of the integrals. However, this does not happen for temperatures up to a few thousands degrees. At large interatomic distances the integrands go smoothly down to zero. With the integration limits taken between 5 and 25 a.u., the integrals in Eq. (12) change by about 1%, which shows that the contribution to the integrals from regions beyond 30 a.u. can be neglected. These conclusions apply to all the integrals over the interatomic distances considered in this work. All the spline fits and numerical integrations needed in this work are performed using MATHEMATICA.[66]

IV. RESULTS AND DISCUSSION

Among the properties studied in the present paper, the isotropic averages of the interaction-induced polarizability and hyperpolarizability are the most sensitive to the choice of the one-particle basis set. In the discussion of the basis set study we therefore focus on the convergence of $\Delta\alpha_{\mathrm{ave}}$ and $\Delta\gamma_{\parallel}$. The series of correlation consistent basis sets x-aug-cc-pVXZ converge for each fixed x-aug level to a valence basis set limit, if the XZ level is increased successively. For γ the fastest convergence is usually obtained in the d-aug or t-aug series;[43,47] higher augmentation levels give usually no further improvements. The results for the interaction-induced second hyperpolarizability $\Delta\gamma_{\parallel}$ converge only slowly with the original correlation consistent basis sets, exemplified by the d-aug-cc-pVXZ series in Table I. The presence of the $(3s3p2d1f1g)$ midbond functions makes the convergence of the x-aug-cc-pVXZ basis sets smoother and faster for the smaller zeta (XZ) levels, although the results obtained at a double zeta (DZ) level are still insufficient.

For $\Delta\gamma_{\parallel}$, the d-aug-cc-pVXZ-33211 series converges from below to a value of approximately 33.6–33.7 a.u., while the t-aug-cc-pVXZ-33211 results approach the same limit from above. For $\Delta\alpha_{\mathrm{ave}}$, the d-aug-cc-pVXZ-33211 and the t-aug-cc-pVXZ-33211 series approach both from below the small value of $\approx$0.01 a.u. As it is seen from the results in Table III, the equilibrium distance (7.10 a.u.) is accidentally close to the point where $\Delta\alpha_{\mathrm{ave}}$ changes its sign.

The calculation of the interaction-induced properties as a function of the internuclear distance in the quadruple and quintuple zeta basis sets would have been rather demanding. Therefore, for the subsequent distance-dependent calculations we chose the d-aug-cc-pVTZ-33211 basis set as a compromise between computational costs and accuracy. From

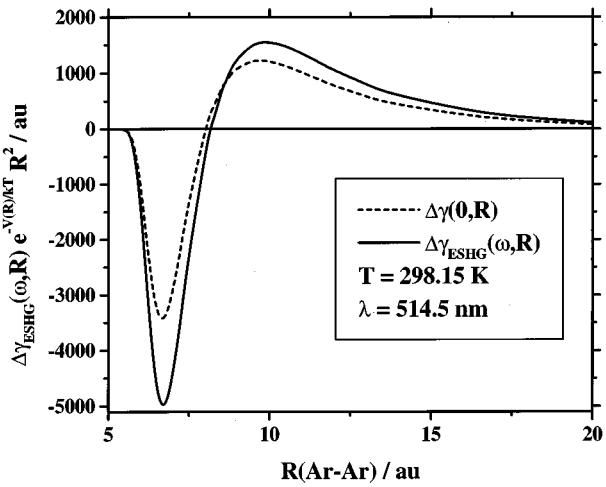


FIG. 4. Ar_2. The function $\Delta\gamma_{\mathrm{ESHG}}(\omega,R)e^{-V(R)/kT}R^2$ (a.u.) against the interatomic distance R (a.u.) for $T=298.15$ K and $\lambda=514.5$ nm.

the results listed in Table II we expect that the basis set error made with this basis set leads for $\Delta\gamma_{\parallel}$ to a curve which in the range 6–12 a.u. is shifted to values which are about 3 a.u. too high compared to results obtained with larger basis sets. For the interaction-induced polarizability, the basis set errors are rather small, 3×10^{-3} a.u. at $R=7.0$ a.u., and decrease with increasing distances. The errors in the interaction-induced changes of the Cauchy moment $\Delta S_{\rm ave}(-4)$ and its counterpart for the second hyperpolarizability $\Delta(\gamma_{\parallel}\times A)$ are larger than the errors in the corresponding static properties, but since the dispersion contributions to the virial coefficients calculated from these properties for the frequencies considered here are about an order of magnitude smaller than the frequency-independent contributions, this does not lead to large errors in the final results.

The curves for three static properties calculated as a function of the internuclear distance: $\Delta\alpha_{\rm ave}$, $\Delta\alpha_{\rm ani}$ and $\Delta\gamma_{\parallel}$ follow the typical shape for interaction-induced polarizabilities and hyperpolarizabilities for atomic dimers.[34,37,67,68] For all three properties the lowest order dispersion contribution parallels the behavior of the corresponding static properties: $\Delta\alpha_{\rm ave}$ and $\Delta S_{\rm ave}(-4)$ start being negative for small distances, reach a maximum at about 8.0 a.u. and decrease then with a $1/R^6$ behavior to zero. The $\Delta\alpha_{\rm ani}$ and $\Delta S_{\rm ani}(-4)$ are positive over the whole range of $R=5-30$ a.u. and decrease monotonically with increasing R; in the long range they fall off as $1/R^3$. The interaction-induced second hyperpolarizability $\Delta\gamma_{\parallel}$ and the lowest order dispersion contribution to this property $\Delta(\gamma_{\parallel}\times A)$ are positive for small distances, decrease to a negative minimum and increase again to a positive maximum before decreasing monotonically to zero, asymptotically as $1/R^6$.

Due to the shapes of the isotropic properties as a function of the internuclear distance, the integrals in $X_{\alpha_{\rm ave}}$, X_K^{γ} and X_{γ} are very sensitive to the balance between the positive and the negative regions in the integrands (see Figs. 1, 3 and 4). The accuracy of the *ab initio* results for the corresponding virial coefficients is thus determined by the accuracy with which this balance is described. An example of how the cancellation between the regions of positive and negative area affects the accuracy of the results of a typical integral, and how critically this depends on the choice of basis set, can be seen in the case of the X_{γ} integral of Eq. (21), computed for instance at $T=298.15$ K and $\lambda=514$ nm (see Fig. 4). In this case the contribution to the integral from the region of negative (~5–8 a.u.) and positive (~8–30 a.u.) areas is roughly $-83\,000$ and $+107\,000$ a.u., respectively, for a balance of $\approx 24\,000$ a.u. To obtain an estimate of how the remaining basis set error might affect this balance, we scaled the curve of the $\Delta\gamma_{\parallel}$ (see Table III) by a factor of $(-40.04)/(-37.46)$ in the region of negative area, and by a factor of 7.98/10.99 in the region of positive area, to approximate the effect of the changing basis set from the d-aug-cc-pVTZ-33211 to the t-aug-cc-pVQZ-33211 (see Table II). The contribution of the two regions changes to $\sim -86\,000$ and $+84\,000$ a.u., respectively, with a resulting balance of ~ -2000 a.u. This corresponds to a change of sign and a decrease of about an order in absolute magnitude in $B_{\gamma}(\omega,T)$ and $b(\lambda=514.5$ nm, $T=298.15$ K). We expect this to be a very conservative error estimate, since the results in the three quintuple zeta basis sets are much closer to the d-aug-cc-pVTZ-33211 value than to the t-aug-cc-pVQZ-33211 value (see Table I). Note that the basis set effect on the balance of positive and negative contributions to the interaction integrals depends on the temperature, as the region of negative area becomes of increasing importance as T increases. Due to the faster convergence of $\Delta\alpha_{\rm ave}$ with respect to the extension of the basis set compared to $\Delta\gamma_{\parallel}$, we expect that the second dielectric and the second refractivity virial coefficients $B_{\epsilon}(T)$ and $B_R(\omega,T)$ are obtained with higher accuracy than the hyperpolarizability virial coefficients B_K^{γ} and B_{γ}. The results for the $B_{\epsilon}(T)$ and $B_R(\omega,T)$ are listed in Table IV and plotted in Fig. 5. For the second dielectric virial coefficient $B_{\epsilon}(T)$ we obtain reasonably good agreement with the available experimental data for the temperature range 242 K$<T<$303 K, in particular when taking into account the large variations of the experimental results. For $T>303$ K, however, the experimental data decrease much faster than the CCSD results. For the second refractivity virial coefficient experimental results are available for $T=296.82$ K[13] and $T=298.2$ K[4,6,8] at a few frequencies and for 323 K[10] at $\lambda=632.99$ nm. The CCSD

TABLE IV. Argon. The second dielectric virial coefficient $B_{\epsilon}(T)$, the dispersion contribution $B_R^{(2)}(T)$ and the second refractivity virial coefficient $B_R(\omega,T)$ at $\lambda=632.8$ nm (T in K, virial coefficients in cm^6 mol^{-2}, with frequencies in a.u.).

T	$B_{\epsilon}(T)$	$B_R^{(2)}(T)$	$B_R(\omega,T)$
242.95	1.4598[a]	5.4882	1.4882
253.00	1.4410	5.4351	1.4691
261.00	1.4268	5.3927	1.4548
273.15	1.4066	5.3281	1.4343
274.00	1.4053	5.3236	1.4329
287.00	1.3852	5.2545	1.4125
293.00	1.3765	5.2226	1.4035
296.00	1.3722	5.2068	1.3992[b]
298.15	1.3691[c,d]	5.1954[e]	1.3961[f,g,h]
303.15	1.3622[i,j]	5.1690	1.3890
305.00	1.3597[k]	5.1592	1.3864
315.00	1.3464	5.1067	1.3728
322.00	1.3374[l,m,n,o]	5.0701	1.3637[p]
340.00	1.3155	4.9768	1.3413
370.00	1.2770	4.7991	1.3019
407.60	1.2449[q]	4.6383	1.2689

[a]Exp., 1.84±0.07, Ref. 11.
[b]Exp., 2.52(34), $\lambda=594.096$ nm—1.73(34), $\lambda=543.516$ nm—1.81(34), $\lambda=325.530$ nm, $T=296.82$ K, Ref. 13.
[c]Calc., 1.53, at 300 K, Ref. 72.
[d]Exp., 0.79±0.10, Ref. 5.
[e]Calc., 9.41, at 300 K, Ref. 72.
[f]Exp., 1.57±0.58, $\lambda=632.8$ nm—1.55±0.74, $\lambda=514.5$ nm—1.58±0.69, $\lambda=488.0$ nm—1.53±0.32, $\lambda=457.9$ nm, $T=298.2$ K, Ref. 8.
[g]Exp., 2.16±0.34, $T=298.2$ K, $\lambda=632.8$ nm, Ref. 4.
[h]Exp., 1.49±0.15, at 298.2 K, $\lambda=632.8$ nm, Ref. 6.
[i]Exp., 1.22±0.09, Ref. 11.
[j]Exp., 1.23±0.05, Ref. 9.
[k]Exp., 1.0±2.1, $T=306.15$ K, Ref. 1.
[l]Calc., (SCF) 0.48, Ref. 37.
[m]Exp., 0.39±0.20, Ref. 2.
[n]0.726 from CIS measurements, Ref. 7.
[o]Exp., 0.72±0.13, at 323 K, Ref. 3.
[p]Exp., 1.76±0.05, $T=323$ K, $\lambda=632.99$ nm, Ref. 10.
[q]Exp., 0.1±0.3, Ref. 11.

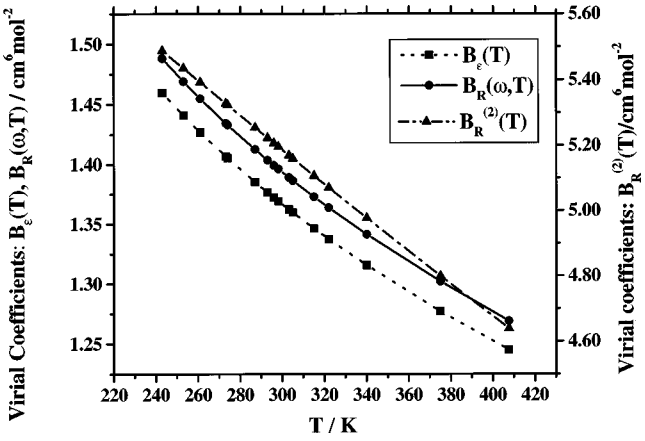


FIG. 5. Argon. Temperature dependence of the second dielectric virial coefficient $B_\epsilon(T)$ of the dispersion contribution $B_R^{(2)}(T)$ and of the second refractivity virial coefficient $B_R(\omega,T)$ computed for $\lambda=632.8$ nm.

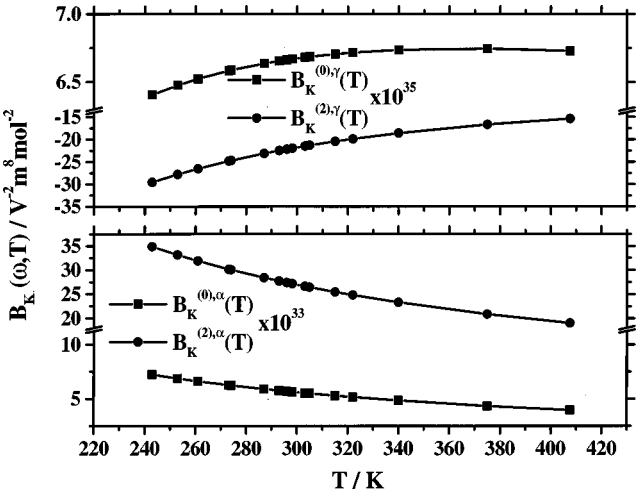


FIG. 6. Argon. The second Kerr virial coefficient $B_K(\omega,T)=B_K^\alpha(\omega,T)+B_K^\gamma(\omega,T)$ as a function of temperature. $B_K^\alpha(\omega,T)=B_K^{(0),\alpha}(T)+2\omega^2B_K^{(2),\alpha}(T)$; $B_K^\gamma(\omega,T)=B_K^{(0),\gamma}(T)+2\omega^2B_K^{(2),\gamma}(T)$.

value for $B_R(\omega,T)$ at 298.15 K is in good agreement with the experimental results of Refs. 8 and 6; the result of Ref. 4 is about 50% higher. The experimental data at 296.82 and 323 K are both larger than that predicted by CCSD.

Comparison with the MP2 second dielectric virial coefficient results of Joslin *et al.*[36] shows that CCSD predicts values which are about one order of magnitude larger than MP2, and about twice as large as the predictions of the spectral model which reproduces the experimental CILS spectrum.[7,69]

Table V and Fig. 6 show the results for the second Kerr virial coefficient $B_K(\omega,T)$. As anticipated in Sec. II, $B_K(\omega,T)$ is dominated by the polarizability contribution $B_K^\alpha(\omega,T)$ which originates from the interaction-induced polarizability anisotropy $\Delta\alpha_{\rm ani}$. For argon, the hyperpolarizability contribution $B_K^\gamma(\omega,T)$ makes only a small correction of about 1%; for the experimentally important frequency range, >450 nm, it is however larger than the dispersion contribution. For $\lambda=458$ nm, our CCSD results for the total second virial Kerr coefficient $B_K(\omega,T)$ are about 25%–45%—twice the experimental error bar—larger than experimental results from Dunmur *et al.*[14] We obtain however better agreement with a recent, very accurate Kerr measurement by Shelton and Palubinskas,[17] who obtained for the ratio $b_{\rm fit}/a_{\rm fit}$ in the virial expansion $\gamma_{\rm eff}^K=a_{\rm fit}+b_{\rm fit}\rho+c_{\rm fit}\rho^2$ a value of $(8.9\pm0.3)\times10^{-5}$ m^3 mol^{-1} at $\lambda=632.8$ nm and $T=296.15$ K. The ratio $b_{\rm fit}/a_{\rm fit}$ measured by Shelton and Palubinskas can be directly compared to the ratio $B_K(\omega,T)/A_K(\omega,T)$ of the second and the first Kerr virial coefficients defined in the expansion [Eq. (14)]. Using the experimental result of Ref. 17 for the dc Kerr hyperpolarizability at 632.8 nm (77.8×10^{-63} C^{4}m^{4}J^{-3}) and our CCSD results for $B_K(\omega,T)$ we obtain for the ratio $B_K/A_K=b_{\rm fit}/a_{\rm fit}$ a value of 9.23×10^{-5} m^{3}mol^{-1}, in very good

TABLE V. Argon. The second Kerr virial coefficient $B_K(\omega,T)=B_K^\alpha(\omega,T)+B_K^\gamma(\omega,T)$. The two contributions are further expanded as $B_K^\alpha(\omega,T)=B_K^{(0),\alpha}(T)+2\omega^2B_K^{(2),\alpha}(T)$ and $B_K^\gamma(\omega,T)=B_K^{(0),\gamma}(T)+2\omega^2B_K^{(2),\gamma}(T)$. The last two columns give $B_K(\omega,T)$ for $\lambda=458$ nm, as computed here and the literature experimental values (T in K, virial coefficients in V^{-2} m^8 mol^{-2}, with frequencies in a.u.).

T	$B_K^{(0),\alpha}(T)$ $\times10^{33}$	$B_K^{(2),\alpha}(T)$ $\times10^{33}$	$B_K^{(0),\gamma}(T)$ $\times10^{35}$	$B_K^{(2),\gamma}(T)$ $\times10^{35}$	$B_K(458\text{ nm},T)$ $\times10^{33}$	$B_K(458\text{ nm},T)$[a] $\times10^{33}$
242.95	7.2289	34.8792	6.4058	−29.5492	7.9776	⋯
253.00	6.8724	33.1552	6.4760	−27.7828	7.5879	5.4±0.9
261.00	6.6134	31.9027	6.5234	−26.5227	7.3049	4.9±0.9
273.15	6.2564	30.1757	6.5831	−24.8213	6.9147	⋯
274.00	6.2330	30.0621	6.5868	−24.7110	6.8890	4.3±0.7
287.00	5.8951	28.4276	6.6360	−23.1477	6.5196	4.0±0.7
293.00	5.7517	27.7333	6.6547	−22.4984	6.3627	3.9±0.7
296.00	5.6827	27.3992	6.6632	−22.1892	6.2872	⋯
298.15	5.6342	27.1648	6.6689	−21.9737	6.2343	⋯
303.15	5.5248	26.6354	6.6813	−21.4911	6.1146	⋯
305.00	5.4855	26.4449	6.6855	−21.3190	6.0716	3.8±0.7
315.00	5.2824	25.4620	6.7052	−20.4438	5.8494	3.8±0.7
322.00	5.1494	24.8178	6.7163	−19.8828	5.7039	⋯
340.00	4.8373	23.3066	6.7356	−18.6100	5.3623	⋯
375.00	4.3310	20.8549	6.7444	−16.6952	4.8080	⋯
407.60	3.9499	19.0089	6.7285	−15.4031	4.3904	⋯

[a]Experimental data from Ref. 14.

TABLE VI. Argon. The second hyperpolarizability virial coefficient. $B_\gamma^{(0)}(T)$, $B_\gamma^{(2)}(T)$ and $b(\omega,T)$ for an ESHG process ($\omega_1=\omega_2=\omega$, $\omega_3=0$, $\omega_L^2=6\omega^2$) at $\lambda=514.5$ nm as a function of temperature (K). To compute b, we assumed $\gamma_\parallel(-2\omega;\omega,\omega,0)=1577$ a.u., as obtained using a t-aug-cc-pV5Z basis set in the recent CCSD study of the hyperpolarizability of the argon atom (Ref. 43). B_γ is given in $C^4\,m^7\,J^{-3}\,mol^{-1}\times10^{-68}$ and b is in $cm^3\,mol^{-1}$. Frequencies are assumed to be given in a.u.

T	$B_\gamma^{(0)}(T)$	$B_\gamma^{(2)}(T)$	$b(\omega,T)$
242.95	7.6288	−35.1908	0.6074
253.00	7.7124	−33.0872	0.6260
261.00	7.7688	−31.5865	0.6389
273.15	7.8400	−29.5603	0.6558
274.00	7.8443	−29.4289	0.6569
287.00	7.9030	−27.5671	0.6718
293.00	7.9252	−26.7939	0.6777
296.00	7.9353	−26.4257	0.6805
298.15	7.9422	−26.1690	0.6825[a]
303.15	7.9569	−25.5943	0.6867
305.00	7.9619	−25.3892	0.6882
315.00	7.9854	−24.3470	0.6956
322.00	7.9985	−23.6789	0.7001
340.00	8.0216	−22.1631	0.7097
375.00	8.0321	−19.8827	0.7217
407.60	8.0131	−18.3439	0.7271

[a]The static value is 0.8074, which can be compared to the estimated value of -29.8 ± 10.8 (Ref. 34) obtained from the *ab initio* result of He and the experimental density ratios of Ref. 12.

agreement with the experiment. Using the CCSD result $\gamma_K(632.8\text{ nm})=1165$ a.u.,[43] which has been calculated with the same basis set as used in the present study for the calculation of the interaction induced properties (d-aug-cc-pVTZ), we obtain for the ratio B_K/A_K a slightly larger result of 9.89×10^{-5} $m^3\,mol^{-1}$. Other reference values in the literature for B_K/A_K are the $(7.5\pm1.2)\times10^{-5}\,m^3\,mol^{-1}$ at $\lambda=632.8$ nm of Ref. 16 and the $(6.3\pm1.2)\times10^{-5}\,m^3\,mol^{-1}$ at $\lambda=457.9$ nm of Ref. 14.

The second virial coefficient B_K is related to the zeroth moment of the depolarized CILS spectrum $M_{\text{depol}}^{(0)}$ which, with the definitions of Ref. 36, coincides with integral $X_K^\alpha(\omega,T)$, [Eq. (17)]. Joslin *et al.*[36] have computed $M_{\text{depol}}^{(0)}$ in the Hartree–Fock and MP2 approximations. Our results are very close to their MP2 estimates, and are thus 15%–20% smaller than both experiment and those derived from the empirical spectral model of Meinander *et al.*[70]

In Table VI and Fig. 7 we have summarized the results for the second virial coefficients of the ESHG hyperpolarizability. As can be expected from the expansion in Eq. (6), the dispersion contribution for the virial coefficients of the ESHG process is much more important than for $B_K(\omega,T)$ and $B_R(\omega,T)$: for ESHG the lowest order dispersion contribution $\omega_L^2 B_\gamma^{(2)}(T)$ accounts at $\lambda=514.5$ nm for approximately 15% of the total second virial coefficient $B_\gamma(\omega,T)$. No experimental data are available that can be compared directly with the present results for $B_\gamma(\omega,T)$. We can, however, combine our CCSD results for argon, $b(\lambda=514.5\text{ nm}, T=298.15\text{ K})=0.68$ $cm^3\,mol^{-1}$, with the static MP4 results for helium from Bishop and Dupuis,[34] $b(0,T)=-1.41\,cm^3\,mol^{-1}$, to obtain a crude estimate for the sum of the coefficients $b(ArH_2)$ and $b(H_2He)$ defined in Eqs. (22) and (23). From Eq. (23) we obtain

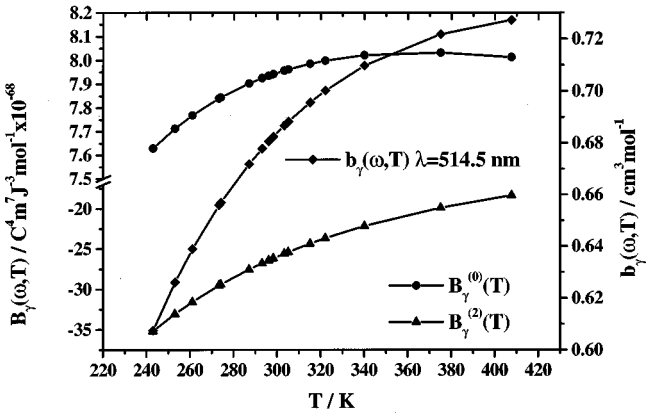


FIG. 7. Argon. Temperature dependence of the second hyperpolarizability virial coefficient, $B_\gamma^{(0)}(T)$, $B_\gamma^{(2)}(T)$ and $b(\omega,T)$, for an ESHG process ($\omega_1=\omega_2=\omega$, $\omega_3=0$, $\omega_L^2=6\omega^2$) at $\lambda=514.5$ nm.

$$b(ArH_2)+b(H_2He)=b_{Ar}\frac{\rho_{Ar}}{\rho_{H_2}}-b_{He}\frac{\rho_{He}}{\rho_{H_2}}. \tag{26}$$

Donley and Shelton[12] measured for $\lambda=514.5$ nm the ratios $\gamma(Ar)/\gamma(H_2)$ and $\gamma(H_2)/\gamma(He)$ as a function of the gas density. The density ratios $\rho_{H_2}/\rho_{Ar}=1.36$ and $\rho_{He}/\rho_{H_2}=14.57$ from this experiment may be combined with our b_{Ar} and Bishop and Dupuis b_{He} to obtain $b(ArH_2)+b(H_2He)=21.0$ $cm^3\,mol^{-1}$. Using the experimental values,[12] $b(ArH_2)=-7.0\pm5.0$ $cm^3\,mol^{-1}$ and $b(H_2He)=+5.6\pm6.2$ $cm^3\,mol^{-1}$, one obtains a value of -1.4 ± 8.0 $cm^3\,mol^{-1}$ for $b(ArH_2)+b(H_2He)$. Taking into account that the experimental estimate carries a large error bar (the uncertainties are treated as single standard deviations) and even considering the remaining error sources in the *ab initio* calculations, there seems to be a reasonable agreement with the mixed MP4/CCSD estimate. Note that even with a change of b_{Ar} as roughly estimated above upon basis set improvement, the result for $b(ArH_2)+b(H_2He)$ changes only by 0.55 $cm^3\,mol^{-1}$, which does not significantly affect the comparison with experiment. However, further experimental and theoretical investigation of the hyperpolarizability dispersion coefficients would be useful to resolve the remaining deviation between the *ab initio* results and experiment.

V. CONCLUSIONS

We report the first CCSD study of the pair interaction-induced static and dynamic electric properties of the argon gas, including the pair contribution to the ESHG and Kerr hyperpolarizabilities. A systematic basis set study shows that the isotropic interaction-induced properties, and in particular $\Delta\gamma_\parallel$, converge only slowly with the one-particle basis sets. The remaining basis set error is therefore expected to be the largest source of inaccuracy in our results. The errors introduced by the approximate treatment of the dispersion contributions and neglect of correlation contributions beyond connected double excitations (CCSD) are expected to be of minor importance. We can provide for the first time high level *ab initio* results for the second refractivity virial coefficient $B_R(\omega,T)$ [including the static limit $B_\epsilon(T)$], the sec-

ond Kerr virial coefficient $B_K(\omega,T)$ and the second hyperpolarizability virial coefficient $B_\gamma(\Omega,T)$ for a broad range of temperatures and frequencies. We find reasonably good agreement with the experimental data for B_ϵ and B_R for $T=242-303$ K. For higher temperatures our calculations predict a much slower decrease of B_ϵ with T than that experimentally reported. Good agreement is also found between the CCSD result for the second Kerr virial coefficient B_K and the results of a recent, very accurate Kerr measurement. Our calculations confirm that $B_K(\omega,T)$ is dominated by the static polarizability contribution $B_K^{(0),\alpha}(T)$; the hyperpolarizability term $B_K^{\gamma}(\omega,T)$ and the lowest-order dispersion correction account only for a few percent of the total value of $B_K(\omega,T)$. Combining our CCSD results for the second virial coefficient for the ESHG process in Ar with a recent MP4 result for the static limit of the coefficient $b(\omega,T)$ of helium, we obtain an estimate for the sum of coefficients $b(\mathrm{ArH_2})+b(\mathrm{H_2He})$ which is in reasonable agreement with the experimental data, although the large error bars associated with the experiment and the remaining sources of error of our *ab initio* study suggest that further efforts are needed in both fields.

ACKNOWLEDGMENTS

One of the authors (C.H.) thanks the European Commission for financial support through the Training and Mobility of Researchers (TMR) program (Grant No. ERBFMBICT 96.1066). B.F. acknowledges grants from the Spanish Direccion General de Ensenanza Superior (Ref. PB95-0861) and the Xunta de Galicia. This work has been supported by the Danish Natural Science Research Council (Grant No. 9 600 856). The authors also thank D. Bishop for discussions.

APPENDIX: CONVERSION FACTORS:

Conversion factors from atomic units to SI:[71]

(i) 1 a.u. of $\rho\equiv a_0^{-3}\,\mathrm{mol}\cong 6.748\,33\times 10^{30}\ \mathrm{m^{-3}\,mol}$;

(ii) 1 a.u. of $\omega\equiv\hbar a_0^{-2}m_e^{-1}\cong 4.134\,14\times 10^{16}\ \mathrm{s^{-1}}$;

(iii) 1 a.u. of $\alpha\equiv e^2a_0^4m_e\hbar^{-2}\cong 1.648\,78\times 10^{-41}\,\mathrm{C^2\,m^2\,J^{-1}}$;

(iv) 1 a.u. of $\gamma\equiv e^4a_0^{10}m_e^3\hbar^{-6}\cong 6.235\,38\times 10^{-65}\ \mathrm{C^4\,m^4\,J^{-3}}$;

(v) 1 a.u. of $A_R(\omega,T)$, $b\equiv a_0^3\,\mathrm{mol^{-1}}\cong 1.481\,35\times 10^{-31}\ \mathrm{m^3\,mol^{-1}}$;

(vi) 1 a.u. of $B_R(\omega,T)\equiv a_0^6\,\mathrm{mol^{-2}}\cong 2.195\,87\times 10^{-62}\ \mathrm{m^6\,mol^{-2}}$;

(vii) 1 a.u. of ${}_mK(\omega,T)$, $A_K(\omega,T)\equiv e^2a_0^9m_e^2\,\mathrm{mol^{-1}}\,\hbar^{-4}\cong 5.604\,08\times 10^{-55}\,\mathrm{V^{-2}\,m^5\,mol^{-1}}$;

(viii) 1 a.u. of $B_K(\omega,T)\equiv e^2a_0^{12}m_e^2\,\mathrm{mol^{-2}}\,\hbar^{-4}\cong 8.304\,39\times 10^{-86}\,\mathrm{V^{-2}\,m^8\,mol^{-2}}$;

(ix) 1 a.u. of $B_\gamma(\omega_0,\omega_1,\omega_2,\omega_3,T)\equiv e^4a_0^{13}m_e^3\,\mathrm{mol^{-1}}\,\hbar^{-6}\cong 9.239\,88\times 10^{-96}\,\mathrm{C^4\,m^7\,J^{-3}\,mol^{-1}}$.

[1] D. R. Johnston, G. J. Oudermans, and R. H. Cole, J. Chem. Phys. **33**, 1310 (1960).
[2] R. H. Orcutt and R. H. Cole, J. Chem. Phys. **46**, 697 (1967).
[3] T. K. Bose and R. H. Cole, J. Chem. Phys. **52**, 140 (1970).
[4] A. D. Buckingham and C. Graham, Proc. R. Soc. London, Ser. A **336**, 275 (1974).
[5] D. Vidal and M. Lallemand, J. Chem. Phys. **64**, 4293 (1976).
[6] R. Coulon, G. Montixi, and R. Occelli, Can. J. Phys. **59**, 1555 (1981).
[7] M. H. Proffitt, J. W. Keto, and L. Frommhold, Can. J. Phys. **59**, 1459 (1981).
[8] R. C. Burns, C. Graham, and A. R. M. Weller, Mol. Phys. **59**, 41 (1986).
[9] T. K. Bose, K. Boudjarane, J. Huot, and J. M. St-Arnaud, J. Chem. Phys. **89**, 7435 (1988).
[10] H. J. Achtermann, G. Magmus, and T. K. Bose, J. Chem. Phys. **94**, 5669 (1991).
[11] J. Huot and T. K. Bose, J. Chem. Phys. **95**, 2683 (1991).
[12] E. A. Donley and D. P. Shelton, Chem. Phys. Lett. **215**, 156 (1993).
[13] U. Hohm, Mol. Phys. **81**, 157 (1994).
[14] D. A. Dunmur, D. C. Hunt, and N. E. Jessup, Mol. Phys. **37**, 713 (1979).
[15] D. A. Dunmur, M. R. Manterfield, and D. J. Robinson, Mol. Phys. **50**, 573 (1983).
[16] A. D. Buckingham and D. A. Dunmur, Trans. Faraday Soc. **64**, 1776 (1968).
[17] D. P. Shelton and J. J. Palubinskas, J. Chem. Phys. **104**, 2482 (1996).
[18] D. P. Shelton, Phys. Rev. A **42**, 2578 (1990).
[19] D. P. Shelton and J. E. Rice, Chem. Rev. **94**, 3 (1994).
[20] V. Mizrahi and D. P. Shelton, Phys. Rev. Lett. **55**, 696 (1985).
[21] D. P. Shelton, J. Chem. Phys. **84**, 404 (1986).
[22] D. P. Shelton, Phys. Rev. Lett. **62**, 2660 (1989).
[23] D. P. Shelton and Z. Lu, Phys. Rev. A **37**, 3813 (1988).
[24] D. P. Shelton and V. Mizrahi, Chem. Phys. Lett. **120**, 318 (1985).
[25] D. P. Shelton, Phys. Rev. A **34**, 304 (1986).
[26] R. E. Cameron and D. P. Shelton, Chem. Phys. Lett. **133**, 520 (1987).
[27] L. Silberstein, Philos. Mag. **33**, 521 (1917).
[28] P. R. Certain and P. J. Fortune, J. Chem. Phys. **55**, 5818 (1971).
[29] A. D. Buckingham and K. L. Clarke, Chem. Phys. Lett. **57**, 321 (1978).
[30] K. L. C. Hunt, Chem. Phys. Lett. **70**, 336 (1980).
[31] L. Frommhold, Adv. Chem. Phys. **46**, 1 (1981).
[32] A. D. Buckingham, E. P. Concannon, and I. D. Hands, J. Phys. Chem. **98**, 10455 (1994).
[33] H. P. Godfried and I. Silvera, Phys. Rev. A **27**, 3008 (1983).
[34] D. M. Bishop and M. Dupuis, Mol. Phys. **88**, 887 (1996).
[35] P. D. Dacre, Mol. Phys. **45**, 17 (1982).
[36] C. G. Joslin, J. D. Goddard, and S. Goldman, Mol. Phys. **89**, 791 (1996).
[37] P. D. Dacre, Mol. Phys. **45**, 1 (1982).
[38] C. Hättig, H. Koch, and P. Jørgensen, J. Chem. Phys. **109**, 3293 (1998).
[39] H. Koch, R. Kobayashi, A. Sanchez de Meras, and P. Jørgensen, J. Chem. Phys. **100**, 4393 (1994).
[40] R. Kobayashi, H. Koch, and P. Jørgensen, Chem. Phys. Lett. **219**, 30 (1994).
[41] C. Hättig, O. Christiansen, H. Koch, and P. Jørgensen, Chem. Phys. Lett. **269**, 428 (1997).
[42] C. Hättig, O. Christiansen, and P. Jørgensen, Chem. Phys. Lett. **282**, 139 (1998).
[43] C. Hättig and P. Jørgensen, J. Chem. Phys. **109**, 2762 (1998).
[44] T. H. Dunning, J. Chem. Phys. **90**, 1007 (1989).
[45] R. A. Kendall, T. H. Dunning, and R. J. Harrison, J. Chem. Phys. **96**, 6796 (1992).
[46] D. E. Woon and T. H. Dunning, J. Chem. Phys. **98**, 1358 (1993).
[47] D. E. Woon and T. H. Dunning, J. Chem. Phys. **100**, 2975 (1994).
[48] D. E. Woon and T. H. Dunning, J. Chem. Phys. **103**, 4572 (1995). The basis sets were obtained from the Extensible Computational Chemistry Environment Basis Set Database, Version 1.0, as developed and distributed by the Molecular Science Computing Facility, Environmental and Molecular Sciences Laboratory which is part of the Pacific Northwest Laboratory, P.O. Box 999, Richland, Washington 99352, and funded by the U.S. Department of Energy. PNL is a multiprogram laboratory operated by Batelle Memorial Institute for the U.S. Department of Energy under Contract No. DE-AC06-76RLO 1830.
[49] J. O. Hirschfelder, W. Byers Brown, and S. T. Epstein, Adv. Quantum Chem. **1**, 255 (1964).
[50] D. M. Bishop, J. Chem. Phys. **90**, 3192 (1989).
[51] B. Fernández and H. Koch, J. Chem. Phys. **109**, 10255 (1998).
[52] S. F. Boys and F. Bernardi, Mol. Phys. **19**, 553 (1970).
[53] C. Hättig, O. Christiansen, and P. Jørgensen, J. Chem. Phys. **107**, 10592 (1997).
[54] C. Hättig and P. Jørgensen, J. Chem. Phys. (submitted).
[55] R. A. Aziz and M. J. Slaman, Mol. Phys. **58**, 679 (1986).
[56] R. A. Aziz, J. Chem. Phys. **99**, 4518 (1993).
[57] A. D. Buckingham and J. A. Pople, Trans. Faraday Soc. **51**, 1029 (1955).
[58] R. Moszynski, T. G. A. Heijmen, and A. van der Avoird, Chem. Phys. Lett. **247**, 440 (1995).

[59] R. Moszynski, T. G. A. Heijmen, P. E. S. Wormer, and A. van der Avoird, J. Chem. Phys. **104**, 6997 (1996).
[60] A. D. Buckingham and J. A. Pople, Faraday Discuss. Chem. Soc. **22**, 17 (1956).
[61] D. A. Kleinman, Phys. Rev. **126**, 1977 (1972).
[62] H. Koch and P. Jørgensen, J. Chem. Phys. **93**, 3333 (1990).
[63] H. Koch, O. Christiansen, P. Jørgensen, A. Sánchez de Merás, and T. Helgaker, J. Chem. Phys. **106**, 1808 (1997).
[64] O. Christiansen, A. Halkier, H. Koch, P. Jørgensen, and T. Helgaker, J. Chem. Phys. **108**, 2801 (1998).
[65] T. Helgaker, H. J. Aa. Jensen, P. Jørgensen, J. Olsen, K. Ruud, H. Ågren, T. Andersen, K. L. Bak, V. Bakken, O. Christiansen, P. Dahle, E. K. Dalskov, T. Enevoldsen, B. Fernández, H. Heiberg, H. Hettema, D. Jonsson, S. Kirpekar, R. Kobayashi, H. Koch, K. V. Mikkelsen, P. Norman, M. J. Packer, T. Saue, P. R. Taylor, and O. Vahtras, DALTON, an *ab initio* electronic structure program, Release 1.0 (1997). See http://www.kjemi.uio.no/software/dalton/dalton.html.
[66] MATHEMATICA, v. 2.1, Wolfram Research.
[67] P. D. Dacre, Mol. Phys. **47**, 193 (1982).
[68] A. D. Buckingham, Pure Appl. Chem. **52**, 2253 (1980).
[69] L. Frommhold and M. H. Proffitt, J. Chem. Phys. **74**, 1512 (1981).
[70] N. Meinander, G. C. Tabisz, and M. Zoppi, J. Chem. Phys. **84**, 3005 (1986).
[71] I. Mills, T. Cvitas, K. Homann, N. Kallay, and K. Kuchitzu, *Quantities, Units and Symbols in Physical Chemistry* (Blackwell Science, London, 1993).
[72] U. Hohm, Z. Naturforsch. Teil A **48a**, 505 (1992).